A Low-cost Fault Corrector for Deep Neural Networks through Range Restriction

Zitao Chen*, Guanpeng Li†, Karthik Pattabiraman*
*University of British Columbia †University of Iowa
{zitaoc, karthikp}@ece.ubc.ca {guanpeng-li}@uiowa.edu

Abstract—The adoption of deep neural networks (DNNs) in safety-critical domains has engendered serious reliability concerns. A prominent example is hardware transient faults that are growing in frequency due to the progressive technology scaling, and can lead to failures in DNNs. This work proposes *Ranger*, a low-cost fault corrector, which *directly rectifies the faulty output due to transient faults without re-computation*. DNNs are inherently resilient to *benign faults* (which will not cause output corruption), but not to *critical faults* (which can result in erroneous output). *Ranger* is an *automated transformation* to selectively restrict the value ranges in DNNs, which reduces the large deviations caused by critical faults and transforms them to benign faults that can be tolerated by the inherent resilience of the DNNs. Our evaluation on 8 DNNs demonstrates *Ranger* significantly increases the error resilience of the DNNs (by 3x to 50x), with no loss in accuracy, and with negligible overheads.

Index Terms—Resilience, Machine Learning, Fault Correction

I. INTRODUCTION

In the recent past, there has been a wide adoption of deep neural networks (DNNs) in various domains [1], [2], [3]. Many of these applications are also safety-critical [4], [5], [6], [7], [8]. One example is autonomous robots, in which DNNs are used for scene understanding and path navigation (e.g., aircraft collision avoidance [4]). Another emerging example is Autonomous Vehicles (AVs), in which DNNs are used to provide end-to-end autonomy. DNNs are crucial for the AV system to perceive its surroundings (e.g., traffic sign detection) in order to safely maneuver the vehicle. Therefore, the safety and reliability of DNNs is becoming a critical consideration.

On the other hand, modern computing systems are becoming increasingly susceptible to hardware transient faults (i.e., soft errors), which often arise due to high-energy particle strikes (e.g., terrestrial neutrons), transistor variability, and thermal cycling. Transient faults typically manifest as *single bit-flips* in the system, and they are predicted to become more frequent due to the effects of technology scaling [9], [10], [11]. Prior studies have shown that transient faults can effectively result in failures of DNNs, leading to safety violations such as causing the AV system to miss obstacles in its path [12], [13]. We refer to these failures as Silent Data Corruptions (SDCs).

Traditional methods to protect systems from soft errors use redundancy at the hardware level (e.g., Triple-Modular Redundancy). However, such techniques are prohibitively expensive, thus making them difficult to deploy in practice. For example, the cost-per-unit and computation performance are of significant importance in many areas (e.g., industrial robotics, AVs). Duplicating hardware components adds to the total cost of the system, and requires synchronization and voting.

There have been many techniques proposed to enhance the error resilience of DNNs [12], [14], [15], [16], [17], [18]. Li *et al.* [12] uses unusual values as symptoms for fault detection [12]. Hong *et al.* proposes to mitigate memory faults by modifying the network's architecture (e.g., using Tanh as activation function) [19]. Mahmoud *et al.* [16] proposes to detect faults based on the mismatch between two duplicated computations. However, these techniques often suffer from limited fault coverage [14], [16], [19] and/or incur significant implementation effort and overhead [12], [14], [16] (more details in Section VII). Moreover, in these systems, program re-execution is often needed in order to recover the correct output. Re-execution incurs considerable overhead and is undesirable for time-critical systems such as AVs that have real-time constraints [20], [21]. Therefore, there is a compelling need for an efficient technique to protect DNNs from transient faults without incurring significant overheads.

To overcome the above challenges, this work proposes *Ranger*[1], a *low-cost* fault correction technique that can *directly rectify the faulty output* due to transient faults without any re-computation. We leverage the insight that DNNs are inherently tolerant of *benign faults* (i.e., faults that will not corrupt the program output in a significant way), and propose *Ranger* to transform the *critical faults* (these are the faults that will result in SDCs) into benign faults. In particular, *Ranger* selectively restricts the ranges of values in specific DNN layers, thereby enabling the DNNs to generate correct output *even in the presence of faults (in most cases)*.

The intuition behind *Ranger* is that DNNs are statistical entities, and *do not* always require exactness in their computations (e.g., incorrect computation of one internal neuron is acceptable if the final predicted label is correct). Thus, range restriction is able to mitigate the large deviation caused by critical faults, so that the reduced deviation can be tolerated by the inherent resilience of DNNs. This eliminates the need to use expensive re-computation to derive the correct results.

We implement *Ranger* as an *automated technique* for the TensorFlow machine learning (ML) framework [22], which is the most widely used ML framework today [23]. *Ranger*

---

[1]Similar to how a park ranger protects parklands, *Ranger* protects DNNs from soft errors by restricting the ranges of values.
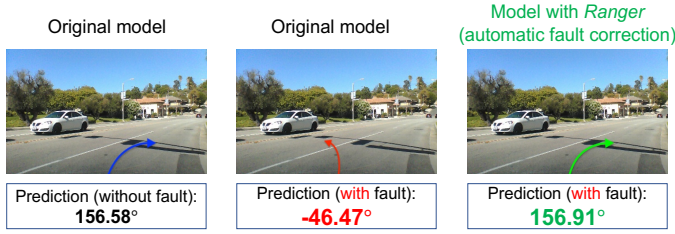
Fig. 1: An example to illustrate how *Ranger* enables automatic fault correction on a DNN deployed in Autonomous Vehicles (AVs).

automatically converts the unreliable DNNs into resilient DNNs, without requiring any programmer intervention.

Fig.1 illustrates how a DNN augmented with *Ranger* can steer an AV in the presence of a transient fault. This is a real example for our experiments. As can be seen, the AV's steering angle changes from $156.58°$ to $-46.47°$ due to a transient fault in the DNN inference. However, *Ranger* performs error correction to restore the faulty value to $156.91°$, which though not exact, is sufficiently close to the original value to navigate the AV safely despite the fault.

Prior work uses value truncation for different purposes in machine learning (ML) domain, such as improving the performance of DNNs [24], [25]; robustness of DNNs to outliers [26], and privacy preservation [27], [28] (Section VII). In contrast, we leverage value restriction for protecting DNNs from transient faults. *Ranger* is based on the idea of our prior work BinFI [13], which distinguishes between benign and critical faults based on the mathematical properties of DNN components, for speeding up fault injections. However, BinFI does not propose any technique to protect the DNNs from the critical faults. *To the best of our knowledge,* Ranger *is the first low-cost technique to provide efficient fault correction for transient faults in DNNs without requiring re-computation.*

The main contributions of this paper are as follows:

- Propose *Ranger*, a technique to selectively restrict the ranges of values in DNNs, which can mitigate the large deviations by critical faults to those that can be tolerated by DNNs. *Ranger* is thus able to rectify the faulty output due to transient faults without performing any re-computation.
- Present an approach to choose particular layers in DNNs for range restriction based on their value dependency, and derive the restriction bounds to be used by *Ranger*.
- Implement *Ranger* in the TensorFlow framework, to automatically make the DNNs resilient to transient faults,
- Perform an experimental evaluation of *Ranger* on 8 DNN models with a total of 5 datasets (including two DNN applications in the AV domain). The evaluation demonstrates that *Ranger*: 1) significantly enhances the resilience of the DNNs models - it reduces the SDC rates from 14.92% to 0.44% (in classifier DNNs), and from 23.76% to 2.49% (in the AV DNNs); 2) does not degrade the accuracy of any of the evaluated models, and 3) incurs negligible memory overheads, and 0.530% performance overhead (on average).

II. BACKGROUND AND FAULT MODEL

In this section, we first provide an overview of deep learning, then describe the reliability challenge for safety-critical DNNs applications like AVs, followed by the fault model.

A. Deep Learning

Deep learning is a field of artificial intelligence that typically leverages DNNs to address problems in both classification and regression. In this paper, we primarily consider convolutional neural networks (CNNs), a class of DNNs application (others such as recurrent neural networks [24] are not considered). A typical DNN uses multiple layers to progressively extract high level features from the raw input. The primary computation usually occurs in the convolution (Conv) layer that extracts the underlying patterns. The results are then fed to the activation (ACT) layer in which the ACT function is used to determine how the neuron should be activated (e.g., performing non-linear transformation). Other layers such as pooling, normalization layers can be added following the ACT layer. The layer closest to the output is usually called fully-connected (FC) layer. An DNN model typically goes through 2 phases: 1) training phase in which the model is trained to learn a particular task or set of tasks; 2) inference phase where the model is used for actual deployment.

B. Reliability of AVs

Autonomous vehicles (AVs) are systems that combine a variety of sensors (e.g., LiDAR) to perceive the surroundings and a control systems (e.g., DNNs) that interpret the sensory information to safely navigate the vehicles such as identifying obstacles in the path. Given the complexity of the road conditions, AVs usually have following requirements: 1) process the humongous sensory information [20], [29] - high throughput; 2) perform real-time action such as applying the brake before collision happens (e.g., an inference rate of 33 ms/frame to classify the frame images) [20], [21] - low latency. These requirements present significant challenges for AV reliability.

Generally, faults in AVs that can result in safety violation (e.g., as per the ISO 26262 standard [30]) can be categorized into systematic faults and transient faults [21]. Systematic faults are induced by design defects in hardware and software, and they can be mitigated at design time [31], [32], [33]. Transient faults, however, need runtime mitigation, which incurs performance overheads. Further, many of these applications have to adhere to standards, e.g., the ISO 26262 standard [30] for AVs requires that there should be no more than 10 FIT (Failure in Time), which is 10 failures in a billion hours of operation. Therefore, it is important to design efficient mitigation techniques for soft-errors that can cause SDCs.

To take one example, a recent study [21] has estimated that an AV needs to classify each frame image in 33 *ms* interval to safely navigate the vehicle. YoLo V5, a state-of-art object detection model released in May 2020, needs 25.5ms for each inference [34], which means the fault protection budget should be lower than 30%; otherwise it could lead to slowdown in response and may result in reaction-time based accidents [35].

Note that this is a conservative estimate as there is variation from frame to frame, and as a safety margin needs to be built in. Therefore, the fault detection and correction should have very low overhead, while having high coverage for SDCs.

C. Fault Model

In this study, we consider hardware transient faults (i.e., soft errors) that occur randomly during the inference phase of the DNNs (the input to the program is correct). We consider the inference phase because DNNs are usually trained once, while the inference tasks are performed repeatedly in deployment, and are hence much more likely to experience faults during their lifetime. Therefore, faults in the inference phase can have severe consequences (e.g., misclassify the "stop" sign as "yield" sign in an AV) [36], [12], [14], [13].

We assume that faults can only arise in the processor's data path (ALUs and pipeline registers); and that the main memory, cache and register file are protected by ECC or parity [37]. Hence, we do not consider faults in these components. This is in line with previous reliability studies [38], [39], [40]. In addition, we assume that faults do not arise in the control logic of the processor, as that constitutes only a small fraction of the total area of the processor. We only consider activated faults as masked faults do not affect the program's execution.

We also assume that at most one fault occurs per program execution, because soft errors are relatively rare events given the typical inference time of DNNs. This also follows the fault models in prior studies [38], [39], [41], [42], [13].

Finally, we inject single bit flips in the software implementation of the DNN, as a transient fault is often manifested as a single bit flip at the software level [43], and studies have shown that multiple bit-flip errors result in similar fault propagation patterns as single bit-flip errors that cause SDCs [44], [45]. With the above said, we also evaluate our work under the multi-bit flip fault model in Section VI-B.

III. METHODOLOGY

To protect the DNNs from transient faults (particularly critical faults), we propose to selectively restrict the ranges of values in different DNN layers. This technique that we call *Ranger*, is based on two properties in DNNs: 1) the monotonicity of operators in DNNs [13]; 2) the inherent resilience of DNNs to insignificant errors [46].

In this section, we first discuss how transient faults result in output corruption in DNNs (e.g., misclassification). We then explain how the characteristics of critical faults in DNNs, and the inherent resilience of DNNs can be leveraged to improve the error resilience of DNNs. Finally, we elaborate on the design of *Ranger* to enable effective fault correction.

A. Fault Propagation in DNNs

Unlike traditional programs in which soft errors can corrupt the outputs by diverting the control flow [38], [47], faults that occur in DNNs are typically numerical deviations (e.g., change of the activation value in the feature map). Even the faults that modify connections between neurons can be modeled
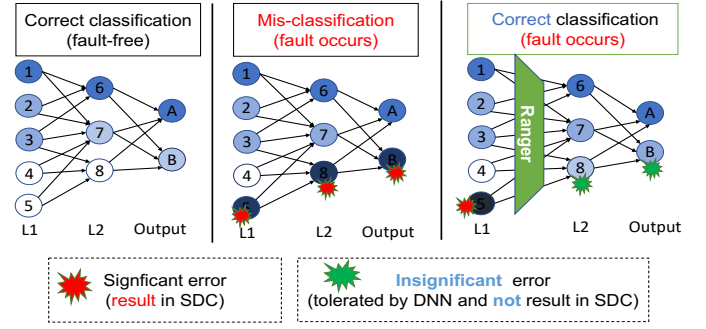

Fig. 2: Example of a fault causing misclassification (SDC), and how *Ranger* enables fault correction by dampening the error to be tolerated by the DNN. Darker colors represent larger values. We assume that label A is the correct label for the DNN under fault-free execution.

as numerical deviations. For example, a fault that causes the DNNs to break the connection between two neurons can be considered as a 0 value passed between them.

The output quality of the DNNs is determined by the numerical output. For classification tasks, the output for the correct label needs to be high, and for the incorrect labels, it needs to be low. For regression tasks, the output needs to be as close to the target variable as possible. Therefore, for a fault to corrupt the output of DNNs, it needs to inflict significantly large deviation at the output.

We provide an example on how a fault could effectively result in a misclassification in an DNN, in Fig. 2. For simplicity, the figure only shows two hidden layers L1 and L2, where the colored nodes denote the activated neurons. The darker nodes are those with larger activation values (e.g., Node 6 has a larger activation value than that of Node 7). Though the fault is propagated through all the subsequent connected neurons, not all of them will result in large deviations - smaller deviations are not highlighted for simplicity (e.g., fault propagating from Node 5 to Node 7 result in small deviations because the weight connection from Node 5 to Node 7 is small).

In the fault-free execution, the classification result is assumed to be correct, i.e., label A. However, when a fault occurs during the computation (Node 5 in the center network in Fig. 2), it causes a large deviation in the faulty neuron, and this subsequently results in the output for label B to be higher than that of label A. This fault thus leads to a misclassification, and is hence a critical fault. *We consider any DNN output that deviates from the correct output of the program as an SDC, e.g., an image misclassification.*

B. Intuition behind Range Restriction

Monotonicity. In prior work, we study the mathematical properties of DNNs, and find that many of the computations in DNNs (e.g., ReLu, SoftMax, multiply-accumulate (MAC)) exhibit the monotone property [13]: *monotonically increasing*: $f(x_i) \geq f(x_j), \forall x_i > x_j$; or *monotonically decreasing*: $f(x_i) \leq f(x_j), \forall x_i > x_j$. For example, assume a fault occurs at the Multiply application in the MAC operation and two faults x_1, x_2 occur at different bits - x_1 is at the high-order

bit. The monotone property is satisfied as: $|x_1 w_i| \geq |x_2 w_i|$, where w_i is the weight. Therefore, the fault propagation effect caused by x_1 is larger than that by x_2 and thus is *more likely* to result in an SDC. This property has been found in the common operations (e.g., Convolution, ReLu, etc.) employed in common DNN architectures (e.g., VGGNet, ResNet) [13].

Thus, the fault propagation behavior can be approximated as a monotone function. This monotone property implies that for faults to cause large deviations at the output layer, they should also cause large deviations at the place where they occur. This leads to the observation that critical faults tend to cluster around high-order bits (i.e., causing large value deviation), while faults at low-order bits tend to be masked and do not typically affect the output much. Thus, range restriction is analogous to "transferring" the faults from the high-order bits to the low-order bits (since the effect caused by fault is reduced), which can be tolerated by the model itself.

Mitigating critical faults. Typically critical faults in DNNs corrupt the output by fault amplification, which would propagate a single fault into multiple values causing large value deviations. Restricting the values in the DNNs reduces the deviations caused by the faults, which in turn lowers the chance of the fault to result in an SDC. This is because DNNs inherently can tolerate small value deviations and generate correct outputs regardless. *Ranger* leverages this property to prevent critical faults from corrupting the outputs, while tolerating other faults. We provide an example in Fig. 2, where the goal of *Ranger* is to reduce the deviation by the critical faults (i.e., significant error) into smaller ones (i.e., insignificant error). Despite the insignificant errors, the system is able to generate the correct output due to the inherent resilience of DNNs. This property enables effective fault correction by *Ranger*, without the need to re-compute the result.

Maintaining the accuracy of original models. While *Ranger* is intended for fault correction, it is also important to ensure that it does not degrade the accuracy of the original models (in the absence of faults). Because *Ranger* derives the restriction bound from the training data (see next section), it is possible for it to truncate some naturally large values in the DNNs. This is especially so when the DNN is tested on unseen data (we use a separate *validation set* that is different from training set to simulate unseen data in our evaluation). We find that though this can occur, it rarely happens in practice as the restriction bound collected from the training data is sufficiently representative of the value ranges (e.g., in the VGG16 model, only in 5 out of 50,000 cases, do the values exceed the restriction bound when the network is tested on unseen data, in the absence of faults). Moreover, even in the above scenario, *Ranger* is still unlikely to degrade the accuracy of the model. This is because *Ranger* only truncates the values to the restriction bound. Such value reduction is often acceptable and can be tolerated inherently by the DNNs, without degrading its accuracy (Section V-B). Note that we do not require the training data to represent the faulty outcomes (unlike in prior work [14], [16]), and hence we do not need to perform expensive fault injection (FI) experiments for *Ranger*.

C. Selective Range Restriction

In this section, we explain how to implement *Ranger* in DNNs. The first step is to *derive the restriction bounds* from the network through profiling, after which the network is transformed to *insert Ranger* on selected layers. Finally, the protected DNN with *Ranger* is released for deployment.

Step 1: Deriving restriction bounds. The restriction bound can be derived from: 1) the function itself, e.g., Tanh function has an inherent bound of $(-1, 1)$: For these functions, we do not have to derive the restriction bounds from the ACT value distribution; 2) Statistical sampling: For functions that are unbounded (such as the ReLu function that does not have an upper bound), the restriction bound can be derived from sampling the distribution of the values in the function, from which we can choose an appropriate bound.

The selection of the bound can be adjusted based on whether we are willing to accept accuracy loss for resilience boosting. A conservative approach is to set the bound to the maximal value such that it is less likely to affect the accuracy of the model. Alternatively, we can also choose a smaller bound to gain higher resilience boosting at the cost of accuracy. We choose the conservative approach as the default configuration, but also evaluate the latter approach (Section VI).

Step 2: Inserting Ranger into selected DNN layers. After deriving the restriction bound, the next step is to apply *Ranger* into the selected layers in DNNs. A DNN typically consists of many different layers [24]: Convolution, Activation (ACT), Pooling, Normalization, Fully-connected layers, etc. While these different layers can be considered for range restriction, we find that range restriction on the ACT layer is particularly desirable for two reasons: 1) ACT function is used to determine the response from the neuron's output (e.g., filtering out the negative output in ReLu ACT function). This particular feature of ACT also makes it ideal to be used for "filtering" out the potential critical faults. For example, an ACT function can restrict a large output from the previous layer (where a transient fault occurs). This restriction reduces the deviation caused by faults, lowering the probability of the fault leading to SDCs. 2) The ACT function is frequently used in different layers in DNNs (e.g., VGGNet, ResNet, etc), and thus applying range restriction on ACT function effectively dampens fault amplification in between layers (as DNNs usually have many layers).

While range restriction in ACT function would limit the fault amplification effect, it is not sufficient as there are still computations that occur between the ACT functions. A single fault in these can quickly propagate and be amplified. For example, consider the following operation in a DNN.

$$y = \text{Relu}_2(\text{Conv}(\text{MaxPool}(\text{ReLu}_1(x)), I)), \qquad (1)$$

where ReLu_1 and ReLu_2 are guarded by *Ranger*. Let their bounds be $bound(\text{ReLu}_1) = 10, bound(\text{ReLu}_2) = 1000$. For simplicity, assume $x = [1, 2]$, and $\text{MaxPool}(\text{ReLu}_1(x)) = 2$. Let the Conv layer have n kernels (we assume that each kernel

is a simple 1x1 identity kernel I), each of which performs a dot-product computation. Thus the dimension of y is $(n, 1)$.

Assume that a fault occurs at MaxPool function and deviates the MaxPool's output from 2 to $1024 + 2$. The faulty value of 1026 subsequently propagates through the Conv layer, and thus *all* the elements from y would be affected. In this case, the fault-free output of y is a n-element vector of 2. *Ranger* can restrict the values from 1026 to 1000 - thus y becomes a vector of 1000. Such a large value deviation has a higher probability of resulting in SDCs. Thus, applying *Ranger* on the ACT layer alone is *not* enough to mitigate critical faults.

By analyzing the value dependency between layers in the model, we find the restriction bound applied to the ACT function can also be *extended* to other functions. Using the same example above, the bound of $ReLu_1$ is also applicable to the MaxPool function, i.e., $bound(\text{MaxPool}(\text{ReLu}_1(x))) = bound(\text{Relu}_1(x))$. Therefore, the values from MaxPool should not be greater than $bound(\text{ReLu}_1) = 10$, and thus y will be a vector of 10 even under the the fault in the MaxPool function, which has a significantly lower deviation (compared with a faulty vector with values of 1000). As a result, the fault is less likely to cause an SDC as the limited deviation can be tolerated by the inherent resilience of DNNs. Therefore, we need to apply range restriction to selected layers beyond just the ACT function to effectively mitigate SDCs.

We describe the procedure of applying *Ranger* to an un-protected DNN in Algorithm 1. The input to the algorithm is the restriction bounds collected from the profiling process (j pair of upper and lower bounds in total for j ACT layers). The resulting output is the DNN protected with *Ranger*. Line 2 traverses each operation in the network. For each of the ACT operations, the output will be bounded (Line 3-4). For all the operations that follow (connect to) the ACT operation and belong to {Max-Pool, Avg-Pool, Reshape, Concatenate}, the *same* restriction bounds will be applied to their outputs as well (Line 5-8). These are the operations where *Ranger* can be deployed beyond the ACT operation (i.e., the operators protected by *Ranger* remain in the same network).

Note that for the Concatenate operation that concatenates the output from the previous 2 ACT operation (this is used in the SqueezeNet model), the restriction bound is derived from the bounds in the preceding 2 ACT operation: lower bound $= \min(low_{j-1}, low_j)$, and upper bound $= \max(up_{j-1}, up_j)$. The time complexity of the algorithm is $O(n)$, where n is the network size (in nodes).

IV. IMPLEMENTATION

We have implemented *Ranger* using the TensorFlow framework [22], which is the most popular framework for writing ML programs today [23]. This allows *Ranger* to be applied to a diverse set of ML programs. In TensorFlow, the program is abstracted as a data-flow graph, which is composed of a set of operators (i.e., different functions). *Ranger* modifies the TensorFlow graph by adding the extra operators for range restriction (tf.minimum and tf.maximum) as per Algorithm 1.

Algorithm 1: Range restriction on DNNs

    Input: $i \leftarrow$ number of operation in the model
             $j \leftarrow$ number of ACT operation
             $(low_j, up_j) \leftarrow$ bounds for the j_{th} ACT op
    Output: Protected DNN with *Ranger*
1: /* Traverse each operation in the network from the first layer to the last one */
2: **for** op_i **in** operations in the network **do**
3:     **if** op_i is the j_{th} ACT operation **then**
4:         Bound op_i with (low_j, up_j)
5:         **if** op_{i+1} **in** {Max-Pool, Avg-Pool, Reshape} **then**
6:             Bound op_{i+1} with (low_j, up_j)
7:         **else if** op_{i+1} **in** {Concatenate} **then**
8:             Bound op_{i+1} with
                $(\min(low_{j-1}, low_j), \max(up_{j-1}, up_j))$
9:         **end if**
10:     **end if**
11: **end for**
12: **return** Protected DNN

We have publicly released the Ranger code under an open-source license (MIT) at the following URL: *https://github.com/DependableSystemsLab/Ranger*

We provide a Python script to *automatically* insert *Ranger* into the DNNs (written as TensorFlow programs). The only inputs needed from the programmer are (1) the restriction bound values, and (2) the name of the activation function such as Relu. The former can be obtained via profiling (Section V-A), while the latter is based on the specific DNN model. Note that it is often trivial to determine the activation function used in a DNN as it is a fundamental design parameter.

Ranger duplicates the TensorFlow graph, and inserts the range checks at the appropriate places, which is then imported into the existing graph. The reason it duplicates the graph is because TensorFlow has a static graph structure and hence the existing operators are not mutable (i.e., the graph is *append-only*). We use TensorFlow's *import_graph_def* functionality for this purpose. We insert the bounded operators via the *input_map* parameter that controls the input mapping relation.

Fig. 3 shows an example. As shown in the left side of Fig. 3, *Relu* is connected as input to the next operator, *MaxPool*. During graph duplication, the output from *Relu* is restricted with *Ranger*, which creates a new operator to be fed as input to the duplicated MaxPool (outlined in green). Each iteration of the duplication process applies *Ranger* in different DNN layers (Algorithm 1). In the example, Step-1 applies *Ranger* on the *Relu* layer and Step-2 applies it on the *MaxPool* layer.

Note that *Ranger* can also be applied to DNNs written in other ML frameworks such as PyTorch. This is because *Ranger* leverages the inherent properties of the DNN model (e.g., the monotone property of the DNN components, the inherent resilience of DNN), which are platform-independent.

V. EVALUATION

A. Experimental Setup

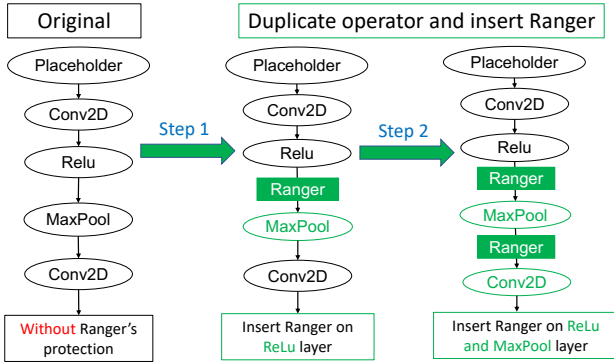**Fault Injection (FI) tool.** Because *Ranger* works on TensorFlow, we use TensorFI [3], an open-source FI tool for

Fig. 3: Illustration of how to automatically deploy *Ranger* on a DNN by duplicating operators (model represented as a data-flow graph).

TABLE I: DNN models and datasets used for evaluation

DNN model	Dataset	Dataset Description
LeNet	MNist	Hand-written digits
AlexNet	Cifar-10	General images
VGG11	GTSRB	Real-world traffic sign
VGG16	ImageNet	General images
ResNet-18	ImageNet	General images
SqueezeNet	ImageNet	General images
Nvidia Dave [53]	Driving	Real-world driving frames
Comma.ai [49]	Driving	Real-world driving frames

TensorFlow-based programs that allows faults to be injected into the TensorFlow graph [48]. We inject random single bit-flip faults directly into the output values of operators in the graph, and observe the final output. This is in line with the FI method in most prior work in the area [14], [12], [13], [48].

Note that we only consider those faults that would not lead to obvious system failures such as a crash (e.g., modifying the dimension of a tensor might cause an error, and terminate the program), as such faults do not result in SDCs.

Hardware: Our experiments were conducted on the following machines: 1) an Ubuntu Linux 18.04.2 system with, 8 RTX 2080Ti GPUs, 24 CPUs with 256 GB memory; 2) a Fedora Linux 20 system, 2 GTX TITAN GPUs, 16 CPUs with 256 GB memory; 3) an Ubuntu Linux 16.04 system with 6 CPUs, 1 GeForce GT610 GPU with 16 GB memory.

Research Questions: We evaluate *Ranger* by asking four research questions (RQs):

RQ1: What is the effectiveness of *Ranger* in fault correction in terms of reducing the SDC rates?

RQ2: Does *Ranger* affect the accuracy of the model?

RQ3: What is the performance and memory overhead associated with *Ranger*?

RQ4: Is *Ranger* effective in DNNs using reduced precision data types?

DNN benchmarks and datasets. In our evaluation, we evaluate DNNs applications in both classification and regression tasks. We consider common DNN classification benchmarks such as VGGNet, SqueezeNet, ResNet. For the DNNs in regression tasks (where the output is a variable value instead of a class label), we choose two DNN applications that can be used in the AV domain - these are the applications that can predict the steering angles of the AV. We choose the Nvidia Dave driving model [8] and the steering model from Comma.ai [49] (which is an AV company). These DNN applications have been adopted in real-world vehicles [50], and are often used as benchmarks for AV studies [31], [13].

We use standard ML datasets such as MNist, Cifar-10, ImageNet), as well as a real-world driving dataset collected from the driving scenes captured by a real vehicle [51].

Table I summarizes the models and datasets in our evalua-

tion. For models using the ImageNet dataset, we report both the top-1 accuracy (i.e., the target label is the predicted class that has the highest probability) and the top-5 accuracy (i.e., the target label is one of the top 5 predictions) [12]. For the two steering models, we use RMSE (root mean square error) and the average deviation per frame to evaluate the model's accuracy - these are also used in other AV DNN studies [52].

Note that FI experiments on DNNs are highly time-consuming - for each input, we need to perform thousands of FI experiments to obtain a statistically significant estimate of the SDC rate. To balance the experimental time with coverage, we choose 10 inputs per model, and ensure that the DNNs are able to generate correct predictions on these inputs (in the absence of faults). We perform 5000 FI trials for each DNN, except for the DNNs using ImageNet, where we perform only 3000 FI trials as they take longer to run (we verified that the results are statistically significant). We also calculated the standard error bars at the 95% confidence level.

In our evaluations, we use 32-bit fixed-point data type for the first 3 RQs (this is more energy-efficient than using a floating-point data type [54]). For RQ4, we evaluate *Ranger* on DNNs using a 16-bit fixed-point data type.

Deriving Restriction Bounds. In our work, we derive the restriction bounds from a randomly-sampled subset of the *training set*. We choose 20% of the training data from each dataset. We find that this is sufficient to derive the ranges for all the DNNs used in our study. For example, Fig. 4 shows the ranges of activation values obtained when sampling different amounts of training data on the VGG16 model. The values are normalized with respect to the global maximal values (i.e., maximal values on all the sampling data). As shown, the value range quickly converges to the global maximal values for all layers. We observe similar trends in the other DNNs, but do not report them due to space constraints.

Note that deriving restriction bounds is a one-time cost, and is *incurred before the deployment of the DNN*. The exact time is dependent on the size of the training data and the network. In our experiments, it took around one hour to complete this process on the largest network (VGG16) in our evaluation with around 20% of training data in the ImageNet dataset.

To reduce *Ranger's* effect on the model's accuracy, we conservatively choose the maximal value observed during the sampling process as the restriction bound (we study the effect of choosing different restriction bounds in Section VI).

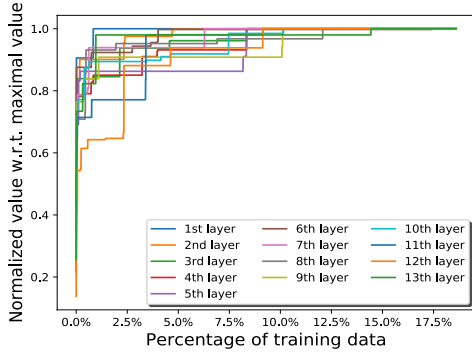---

[3]https://github.com/DependableSystemsLab/TensorFI

Fig. 4: Ranges of values observed in each ACT layer using different amount of data on the VGG16 network (13 ACT layers in total). A total of 186056 images (around 20% of the training set) were used.
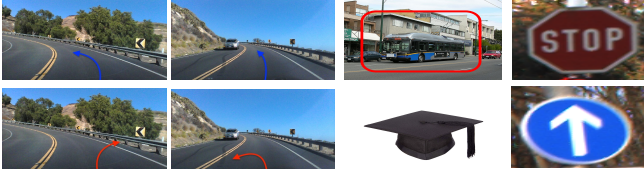

Fig. 5: Examples of SDCs in different DNNs in our evaluation. The first row shows the input to the DNN, the second row shows the corresponding output produced by the DNN under faults.
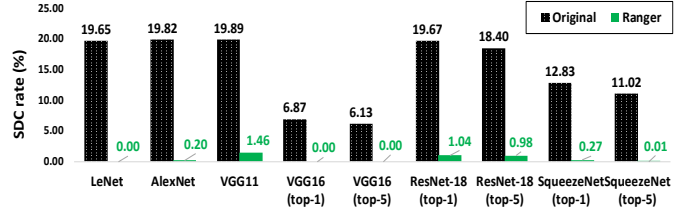

Fig. 6: SDC rates of the original classifier models, and models protected with *Ranger*. For the models using ImageNet, we show the results for top-1 and top-5 accuracy. Error bars range from $\pm 0.04\%$ to $\pm 1.46\%$ at the 95% confidence interval. Lower values are better.
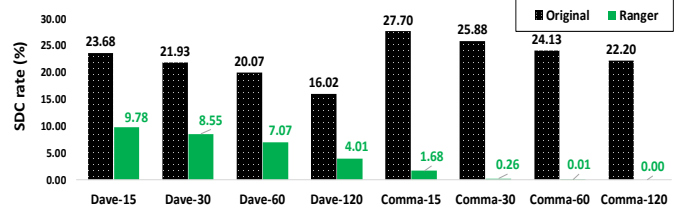

Fig. 7: SDC rates of the original steering models, and models protected with *Ranger*. An SDC is determined based on different thresholds of the degrees of deviation to the correct steering angles (15, 30, 60, and 120 degrees). Error bars range from $\pm 0.03\%$ to $\pm 1.24\%$ at the 95% confidence interval. Lower values are better.

B. Results

RQ1: Effectiveness of range restriction. We measure the *SDC rate*, which is the percentage of the transient faults that cause SDCs, with and without *Ranger*. For classifier models, an SDC will manifest itself as an image misclassification. For the two steering models that produce continuous values as outputs, we use different threshold values for the deviations of steering angles to identify SDCs, namely 15, 30, 60 and 120 degrees as done by our prior work [13]. Fig. 5 illustrates the effect of SDCs in different DNNs tasks from our experiments.

Though *Ranger* selectively applies range restriction on a subset of operations in the DNN, we consider faults that can arise randomly in *all* the operations during the computations except the last FC layer. We exclude the last FC layer because values in this layer are directly associated with the final outputs. Thus, restricting the values in the last FC layer is not effective in mitigating SDCs (we validated this in our experiments). However, the state space of the last FC layer constitutes a very small fraction of the state space (e.g., in VGG16 model, the last FC layer only accounts for 0.0047% of the state space), and techniques such as duplication can be used to protect this particular layer with minimal overheads.

Fig. 6 illustrates the SDC rates in the 6 classifier models with and without *Ranger*. While different DNNs exhibit different SDC rates, Fig. 6 shows that *Ranger* achieves significant SDC reduction across all the models. For example, in the LeNet model, the SDC rate decreases from around 20% to 0% (in our experiments). *On average,* Ranger *reduces the SDC rates from* 14.92% *to* 0.44% *across the models.*

The results from the two steering models are shown in

Fig. 7. In the Comma steering model, *Ranger* can reduce almost all the deviations of steering angles due to transient faults, and completely eliminate large deviations (e.g., 0% of SDCs in the category of threshold=120). However, *Ranger* achieves less pronounced SDC reduction in the Dave model. This is because the Dave model outputs the steering angle in radians, while the Comma model outputs the steering angle in degrees. The conversion from degrees to radians is more sensitive to deviations. The reason is that the conversion function (Atan function in TensorFlow) is horizontal asymptote ($y \in (-\pi/2, \pi/2)$), and thus even a small deviation at the input of Atan function would cause a large output deviation, i.e., higher SDC probability. Based on this observation, we train a new model which outputs the steering angle in degrees instead of radians, which achieves both *better accuracy and better resilience* with *Ranger* than the original model (Section VI).

Quantitative Comparison with related work. Hong *et al.* [19] suggest a defense mechanism against memory bit-flips by modifying the ACT functions of the models such as changing ReLu into Tanh (a similar approach is also proposed in [15]). We compare *Ranger* with the method in Hong *et al.* for 5 of the 8 DNNs. The models we consider are: LeNet, AlexNet, VGG11, Dave and Comma steering model. We only consider these 5 models as we need to train a new model for each DNN, and it is time consuming to do so for the other 3 DNNs.

For both approaches, we report the SDC rate reduction relative to the original SDC rates in Fig. 8 (for brevity, we report the average results for the steering models across all the thresholds). Fig. 8 shows that the approach from Hong *et al.* achieves 0% relative SDC reduction in models using the Tanh activation function. This is because transient faults could occur
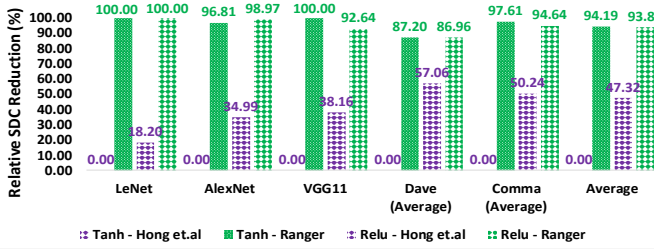
Fig. 8: SDC rate reduction by protecting the DNN with the approach in Hong *et al.* [19] and *Ranger*. Error bars range from $\pm 0.12\%$ to $\pm 1.38\%$ at the 95% confidence interval. Higher values are better.

after the Tanh function in the network, and these would not be affected by the replacement. In contrast, *Ranger* achieves significant SDC reduction because it performs selective range restriction in the entire DNN.

For models using the ReLu function, while both approaches can reduce SDC rates, *Ranger* enables significantly higher resilience boosting than Hong *et al.*. For example, when $threshold = 120$ in the two steering models, the SDC rates in Hong *et al.* vary from 4.76% to 9.48%, while with *Ranger*, the SDC rates vary from 0% to 0.27%, which is *an order of magnitude* lower. On average, *Ranger* achieves *more than 90% SDC rate reduction than Hong* et al. across all the models.

> *Ranger* reduces the SDC rate from 14.92% to 0.44% (34X reduction) for the 6 classifier DNNs, from 24.98% to 0.49% on the Comma.ai model (50X reduction), and 20.42% to 7.35% (2.77X reduction) on the Dave model.

RQ2: Accuracy. In this RQ, we investigate whether the value truncation by *Ranger* affects the accuracy of the DNNs in the absence of faults. We follow the common practice in ML studies to *separate the training and validation set*. The latter is a set of data used for simulating the unseen data, and for evaluating the model learned from the training set. Because *Ranger* derives the restriction bounds from a subset of the *training set*, we choose to evaluate the models on the *validation set*. We compare the accuracy of the original models both with and without *Ranger* on the validation set, in the absence of faults. The results are presented in Table II.

Our results show that applying *Ranger* does not degrade the accuracy of the baseline models in any of the 8 DNNs. This is because the restriction bounds derived from existing data are sufficient to characterize the ranges of values in the DNN (Figure 4). For the rare cases where the normal values exceed the restriction bounds, the value reduction due to *Ranger* does not affect the accuracy.

In the SqueezeNet model, applying range restriction marginally increases the accuracy of the model. This is because the large value corresponding to the incorrect label is reduced by *Ranger*, and thus the classification probability of the incorrect label also decreases.

TABLE II: Accuracy of original DNN, and the DNN protected with *Ranger*. $+$ indicates accuracy improvement. Higher values are better.

DNN model	w/o *Ranger*	w/ *Ranger*	Diff.
LeNet	99.20%	99.20%	0.00%
AlexNet	82.14%	82.14%	0.00%
VGG11	99.74%	99.74%	0.00%
VGG16 (top-1)	64.72%	64.72%	0.00%
VGG16 (top-5)	85.736%	85.736%	0.00%
ResNet-18 (top-1)	62.66%	62.66%	0.00%
ResNet-18 (top-5)	84.61%	84.61%	0.00%
SqueezeNet (top-1)	52.936%	52.940%	+0.004%
SqueezeNet (top-5)	74.150%	74.154%	+0.004%
Dave (RMSE)	9.808	9.808	0.000
Dave (Avg. Dev.)	3.153	3.153	0.000
Comma (RMSE)	24.122	24.122	0.000
Comma (Avg. Dev.)	12.640	12.640	0.000

TABLE III: Time taken to automatically insert *Ranger* in the models.

DNN	Insertion time	DNN	Insertion time
LeNet	3 sec	ResNet-18	22 sec
AlexNet	2 sec	SqueezeNet	11 sec
VGG11	7 sec	Dave	2 sec
VGG16	320 sec	Comma	1 sec

> *Ranger* does not degrade the accuracy of any of the evaluated DNN models in our experiments.

RQ3: Overhead. There are two sources of overhead due to *Ranger*: (1) instrumentation overhead, and (2) runtime overhead. The instrumentation overhead is an one-time effort incurred before the model deployment, while the runtime overhead is incurred during the deployment of the model.

We first measure instrumentation overhead to automatically insert *Ranger* into the models. The instrumentation time for each model is shown in Table III (on a MacBook Pro laptop with 2.3 GHz Intel Core i5 and 16 GB memory). Overall, *Ranger* takes an average of 46 seconds for instrumentation.

We measure the runtime overhead of *Ranger* in terms of its memory and performance overheads during the inference phase. The memory overhead comes from the storage for the restriction bounds, which is proportional to the number of ACT functions in the models (the restriction bounds are applicable for not just ACT functions, but also others such as MaxPool function). Given the typical size of DNNs, this overhead is negligible (e.g., VGG16 has a size of over 500MB).

For the runtime performance overhead, we first measure the absolute runtime of the DNN models. The average inference time across all the models (using GPUs) is 9.41 milliseconds (without *Ranger*) and 9.64 milliseconds (with *Ranger*), with $\pm 0.11\%$ standard deviation. Note that the above runtime is highly dependent on the hardware architecture and system configuration. Therefore, for reproducibility purposes, we measure the performance overhead of *Ranger* in terms of the floating-point operations (FLOPs) incurred by it (using TensorFlow's profiler). FLOPs is a measure of the latency and energy consumption of ML models [55], [56], [57], and is

TABLE IV: Computation overhead of *Ranger* measured in FLOPS. M stands for Million; B stands for Billion.

DNN model	w/o *Ranger*	w/ *Ranger*	Overhead
LeNet	24.622M	24.724M	0.412%
AlexNet	11.361M	11.484M	1.082%
VGG11	87.057M	87.326M	0.309%
VGG16	309.604B	309.905B	0.097%
ResNet-18	36.354B	36.404B	0.138%
SqueezeNet	530.813M	539.215M	1.583%
Dave	56.545M	56.764M	0.387%
Comma	17.673M	17.714M	0.235%

Fig. 9: SDC rate of DNNs using a 16-bit fixed-point data type, with and without *Ranger*. Error bars range from $\pm 0.04\%$ to $\pm 1.33\%$ at the 95% confidence interval. Lower values are better.

TABLE V: Accuracy of the Dave model with different restriction bounds of *Ranger*. 100% is the original. Lower values are better.

Accuracy	Original	100% Bound	99.9% Bound	99% Bound	98% Bound
RMSE	6.069	6.069	8.5719	12.370	13.940
Avg. Deviation	2.651	2.651	2.883	4.077	4.884

independent of the platform.

The results are reported in Table IV. We did not observe variations across different inputs as they all have the same dimension. We find that the overhead of *Ranger* to be very low (0.530% on average) - this is negligible in most cases. This is because *Ranger* only involves range checking and truncation, which are relatively simple operations, compared to the typical operators in a DNN such as convolution.

> *Ranger* incurs negligible performance and memory overheads on average across the DNN models.

RQ4: Effectiveness of *Ranger* under reduced precision data type. In previous RQs, we used a 32-bit fixed-point data type, which is more energy-efficient than a floating-point data type. The data type precision can be reduced to gain further energy efficiency [54]. Therefore, we study the effectiveness of *Ranger* in DNNs using 16-bit fixed-point data type, which can be used for inference in large DNNs. Using smaller data types such as 8-bit datatype cannot provide sufficient dynamic value range for large DNNs [54], and hence we do not study these. Nevertheless, data quantization with lower bit widths is similar to using standard fixed-point datatypes without quantization (e.g., a quantized 8-bit datatype represents comparable range as an unquantized 16-bit datatype). Thus, we posit that *Ranger* will still be effective on them because the observation that the critical faults needs to yield large deviation is independent of the implementation. We use 14 bits for the integer and 2 for the fractional part, which is sufficient for common DNNs [54].

As before, we report the SDC rates of the models with and without *Ranger* in Fig. 9. As shown, *Ranger* is effective in reducing the SDC rate of all 8 DNNs, from 15.11% to 0.93% (a 16X reduction) even with reduced precision data types.

VI. DISCUSSION

In this section, we study the trade off between accuracy and resilience in *Ranger*, then the effectiveness of *Ranger* under multi-bit flips, and finally the design alternatives for *Ranger*.

A. Trade-off between Accuracy and Resilience.

We study how to adjust the restriction bound to gain additional resilience at the cost of accuracy (e.g., in systems that are more prone to transient faults). We focus on the Dave
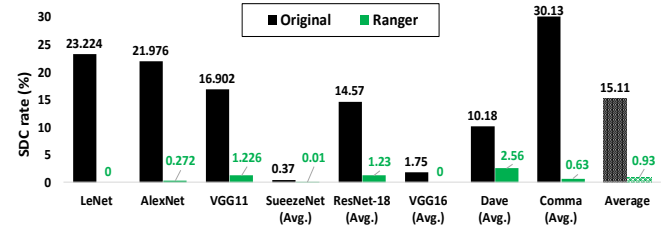
steering model because as shown in Fig. 7, the average SDC rate is around 7% even when it is protected with *Ranger*.

As mentioned, *Ranger* does not yield significant SDC reduction on the original Dave model that outputs the radian value. Therefore, we train a new Dave model whose output is the steering angle in degrees. We then evaluate both the accuracy and SDC rate of the model using different restriction bound values. As mentioned in Section III, we collect the distribution of ACT values from statistical sampling, and can choose the restriction bound accordingly. For example, setting the restriction bound to the 100th percentile means we use the value that covers *all of the sampled values* (i.e., the maximum value) - this was our earlier approach in Section V.

Fig. 10 shows the SDC rates of the model with different restriction bound percentiles, and Table V shows the corresponding accuracy values. As can be seen, the SDC rate reduction due to *Ranger* is higher than that in Fig. 7, leading to a lower SDC rate with *Ranger*. For example, when applying *Ranger* in both models, the SDC rate for the category of *threshold=120* is 4.01% in the original Dave model, and 2.23% in the new model. Also, *Ranger* does not degrade the accuracy of either model. In fact, the accuracy of the new Dave model is higher than that in Fig. 7. This is because the new model outputs the steering angle in degrees, which has a larger dynamic range than radian values, thereby allowing the model to make more accurate predictions.

As expected, setting a restriction bound to a lower-percentile value boosts the resilience, but also degrades the accuracy of the models. When comparing the models using 100% bound and 99.9% bound, the average deviation per frame increases from 2.651 to 2.883. However, this provides a higher resilience boost, e.g., the SDC rate for $threshold = 120$ reduces from 2.23% to 0.27%. On average, choosing the 99.9% percentile restriction bound reduces the SDC rate from 22.54% to 2.9% (7.7x reduction), for this model, with marginal accuracy loss.
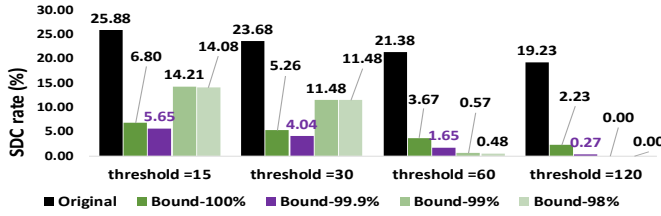
Fig. 10: SDC rates for the Dave model protected by *Ranger* for different restriction bounds. Error bars range from $\pm 0.14\%$ to $\pm 1.39\%$ at the 95% confidence interval. Lower values are better.
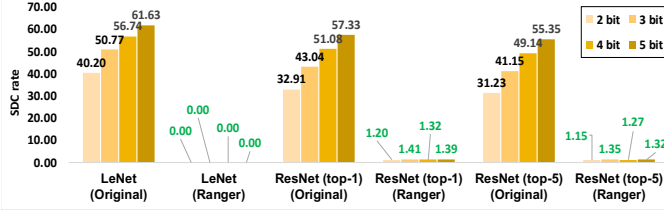

Fig. 11: SDC rates for the classifier models (with and without *Ranger*) under multi-bit flips. Numbers in green are the SDC rates of models protected by *Ranger*. Error bars range from $\pm 0.38\%$ to $\pm 1.79\%$ at the 95% confidence interval. Lower values are better.

B. Fault Correction for Multi-bit Flips

We now evaluate the effectiveness of *Ranger* under the multi-bit flip fault model. Note that multi-bit flips can manifest either as multiple, independent [44] bit-flips (i.e., in multiple values), or as consecutive bit-flips [58] (i.e., in the same value). We assume the former model, namely multiple, independent bit-flips, as this will potentially result in *more* values being affected by the fault. Therefore, our analysis is conservative.

We hypothesize that *Ranger* will continue to be effective as it is agnostic to the number of out-of-bound values, as it restricts *all* the values that exceed the restriction bound. To test this hypothesis, we conducted experiments on two of the classifier models (LeNet and ResNet) and the two DNN models used in AVs. We inject multiple-bit flips (ranging from 2 bits to 5 bits) at randomly chosen values. These multi-bit faults can affect *multiple* data values - thus, they are more potentially damaging as more values will be corrupted by faults. As before, we inject 3000 faults per input per model.

The results are shown in Fig.11 and Fig.12. As shown, the SDC rates of the original models increase with the number of multi-bit flips without *Ranger*. However, with *Ranger*, the SDC rates are significantly lower, in all cases. Further, the SDC rates for the classifier models protected by *Ranger* remain relatively constant with the number of bit-flips, while the SDC rates in the AV DNNs protected by *Ranger* increase with the number of bit flips (though at a slower rate than without *Ranger*). This is because the AV DNNs output the steering angle value, which require exactness (unlike classifier models).

Overall, with multiple bit-flips, the average SDC rate is reduced from 47.55% to 0.87% (55X reduction) for classifier DNNs; and 58.38% to 6.97% (8.4X reduction) for AV DNNs.
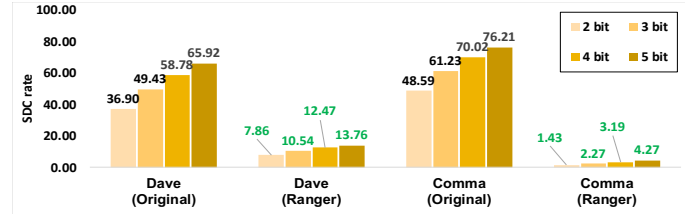

Fig. 12: SDC rates for the AV DNN models (with and without *Ranger*) under multi-bit flips. Numbers in green are the SDC rates of the models protected by *Ranger*. Error bars range from $\pm 0.43\%$ to $\pm 1.79\%$ at the 95% confidence interval. Lower values are better.

C. Design Alternatives for Ranger

While *Ranger* restores out-of-bound values to the restriction bound, we explore other design alternatives for *Ranger* based on other work. For example, Reagen *et.al* propose to reset the faulty value to 0 upon the detection of a fault [59]. Similarly, we can restrict all the out-of-bound value to 0, instead of the restriction bound. We conduct a targeted experiment on the VGG16 model using this strategy. We observe that resetting values beyond the bound to 0 significantly degrades the accuracy of the original model (e.g., $3/5 = 60\%$ of the inputs are inaccurate after the resetting). This is because the value reduction is so drastic that the model is not able to generate a correct output. Further, resetting the values to 0 is likely to cause 0 values in subsequent operations in the network, such as multiplication, which can lead to incorrect results.

Another possibility is to replace out-of-bound values with a random value between 0 and the restriction bound. We perform another experiment where we reset the values outside the restriction range to random values (within the restriction bound) - we inject 1000 faults for this experiment. Even though some of the classification results change (where the incorrectly predicted labels change), the top-1 and top-5 accuracies remain the same. Therefore, random replacement is also a viable strategy, though *Ranger* is much more deterministic and may be preferred for safety-critical systems such as AVs.

VII. RELATED WORK

Assessing the reliability of DNNs: Assessing the resilience of a system is often the first step towards protecting it. Therefore, there has been a plethora of work aiming to understand the reliability of DNNs via FI. Li *et al.* assess the resilience of the DNNs by randomly injecting transient faults into the DNN accelerator [12]. Reagen *et al.* perform FI into the DNNs systems to study the trade off between model accuracy and fault rate [36]. Santos *et al.* study the resilience of ML application under mixed-precision architectures [60]. In prior work, we propose a binary FI technique to effectively identify the critical faults in DNNs, based on the mathematical property of the DNNs' components [13], i.e., its monotonicity (similar to *Ranger*). While these studies provide insights into the ML applications' resilience, they do not mitigate the faults.

Improving the reliability of DNNs: Several techniques have been proposed to enhance the error resilience of DNNs [12],

[14], [15], [17], [18]. Mahmoud *et al.* [16] use statistical FI to identify vulnerable regions in DNNs, and selectively duplicate the vulnerable computations for fault detection. However, their approach incurs high computational overheads. Li *et al.* [12] leverages the value spikes in the neuronal responses as the symptoms for fault detection. However, this technique has a false-positive rate of over 30%, and program re-execution is required to restore the correct output. Schorn *et al.* [14] builds a supervised learning model to distinguish between benign and critical faults in DNNs, as well as perform error correction. However, their technique requires extensive FI, which is particularly time-consuming for large DNNs. For example, for a single input in the VGG16 model, there could be over 30 million values that can be corrupted by faults. Therefore, performing FIs to obtain a comprehensive training set is prohibitively expensive for large DNNs.

Hong et al. [19] propose an approach to mitigate memory faults in DNNs by modifying the DNN architecture, e.g., using Tanh as the activation function, which is different from *Ranger*'s focus is on mitigating computational faults. Though they focus on memory faults (which is assumed to be protected by ECC in our work), we evaluate whether the proposed technique [19] is effective against computational faults as well. However, our evaluation in Fig. 8 shows that this is not the case. Techniques based on Algorithm-based Fault Tolerance (ABFT) have also been proposed for detecting faults in particular layers in DNNs (e.g., Conv layer [17], [18], [61]; matrix multiplication [62]). However, these techniques do not provide protection for faults arising in other areas of the DNN, and for the fault propagating into multiple neurons.

Our work differs from these papers in the following ways:

- *Ranger* uses value restriction in different DNN layers as a way to rectify the faulty outputs due to transient faults. The other papers focus on fault detection [12], [16], [17]; they resort to black-box ML [14] or redundancy [16] to protect the ML program from transient faults.
- *Ranger* is an automated transformation that can be integrated into existing DNNs with minimal effort. In contrast, other work often require significant effort (e.g., perform expensive FI prior to deployment [14], [16]).
- *Ranger* is highly effective in fault correction with negligible overhead. We provide a comparison with representative works in Table VII. As can be seen, existing techniques in Table VII all suffer from either low SDC coverage or high performance overhead. In contrast, *Ranger* achieves an SDC coverage of over 97% with around 0.5% overhead, which significantly outperforms existing techniques.

Approximate computing in ML: Many studies have used approximate computing techniques to lower the computation demands for DNNs [46], [54], [63]. Leveraging the resilience of DNNs to inexactness in the computations, these studies propose to identify those neurons that have low impact on the final output. They then either replace them with an approximate low-precision design [46] or even remove them altogether [63]. While our study also exploits the inherent

TABLE VI: Comparison of *Ranger* with existing techniques on protecting DNNs from hardware transient faults.

Technique	SDC coverage	Overhead
Triple Modular Redundancy	100%	200%
Selective duplication [16]	∼60%	30%
Symptom-based detector [12] [1]	99.5%	74.48%
ML-based error corrector [14]	66.95%	0.95%
Hong *et al.* [19][2]	31.54%	0%
ABFT-based approach [17] [3]	29.98%	< 8%
***Ranger* (Ours)**	**97.05%**	**0.53%**

[1] Li *et al.* [12] did not report overhead numbers, and so we re-implemented their technique with our best effort, and measured them.
[2] Results are based on the evaluation in Fig. 8. The approach in Hong *et al.* does not incur any overhead as it modifies architecture itself such as replacing the activation function with another one.
[3] Zhao *et al.*[17] injected faults only into the convolution layer. So we estimated their overall coverage based on the proportion of faults in the convolution layer compared to the entire network.

resilience of DNNs, we restrict the ranges of values in selected DNN layers rather than find sensitive neurons in the DNNs.

Value truncation in ML: Value truncation has been widely used in the ML domain for various purposes (e.g., performance [24], [25]; robustness to outliers [26]; privacy [27], [28]). Gradient clipping is used to address gradient explosion during the training of DNN by rescaling the gradients to a certain range [24]. The loss function of the model can also be applied with truncation to improve the robustness of the learning algorithm [26]. Unlike these papers, we use range restriction to enable efficient (transient) fault correction.

Adversarial attack against ML: While our work studies how to rectify output corruption due to hardware transient faults, such failures can also be induced by manipulating the inputs to the ML models via adversarial attacks [64]. Our fault model (Section II-C) assumes that the inputs to the models are uncorrupted, and hence we do not consider adversarial attacks.

VIII. CONCLUSION

In this work, we propose *Ranger*, an automated fault correction technique that selectively restricts the ranges of values in particular DNN layers, in order to dampen the large deviations typically caused by transient faults leading to Silent Data Corruptions (SDCs). The reduced deviations can be tolerated by the inherent resilience of DNNs, without causing SDCs. *Ranger* is an automated transformation that can be integrated into existing DNNs with minimal programmer effort.

We evaluate *Ranger* on 8 popular DNN models, 6 of which are classifiers, and two are steering models used in the AV domain. Our evaluation demonstrates that *Ranger* can reduce the SDC rates of the classifier DNNs from 14.92% to 0.44%, and those of the steering models from 23.76% to 2.49%, without degrading the accuracy of any of the original models, and incurring negligible memory and performance overheads.

As future work, we plan to (1) explore the combination of *Ranger* with existing techniques such as ML-based approaches, to reduce the remaining margin of SDCs, and (2) extend *Ranger* to other ML frameworks than TensorFlow.

REFERENCES

[1] T. B. Brown, B. Mann, N. Ryder, M. Subbiah, J. Kaplan, P. Dhariwal, A. Neelakantan, P. Shyam, G. Sastry, A. Askell *et al.*, "Language models are few-shot learners," *arXiv preprint arXiv:2005.14165*, 2020.

[2] K. He, X. Zhang, S. Ren, and J. Sun, "Deep residual learning for image recognition," in *Proceedings of the IEEE conference on computer vision and pattern recognition*, 2016, pp. 770–778.

[3] A. Krizhevsky, I. Sutskever, and G. E. Hinton, "Imagenet classification with deep convolutional neural networks," in *Advances in neural information processing systems*, 2012, pp. 1097–1105.

[4] K. D. Julian, J. Lopez, J. S. Brush, M. P. Owen, and M. J. Kochenderfer, "Policy compression for aircraft collision avoidance systems," in *2016 IEEE/AIAA 35th Digital Avionics Systems Conference (DASC)*. IEEE, 2016, pp. 1–10.

[5] Z. Xiong, M. K. Stiles, and J. Zhao, "Robust ecg signal classification for detection of atrial fibrillation using a novel neural network," in *2017 Computing in Cardiology (CinC)*. IEEE, 2017, pp. 1–4.

[6] P. Rajpurkar, A. Y. Hannun, M. Haghpanahi, C. Bourn, and A. Y. Ng, "Cardiologist-level arrhythmia detection with convolutional neural networks," *arXiv preprint arXiv:1707.01836*, 2017.

[7] A. Esteva, B. Kuprel, R. A. Novoa, J. Ko, S. M. Swetter, H. M. Blau, and S. Thrun, "Dermatologist-level classification of skin cancer with deep neural networks," *Nature*, vol. 542, no. 7639, p. 115, 2017.

[8] M. Bojarski, D. Del Testa, D. Dworakowski, B. Firner, B. Flepp, P. Goyal, L. D. Jackel, M. Monfort, U. Muller, J. Zhang *et al.*, "End to end learning for self-driving cars," *arXiv preprint arXiv:1604.07316*, 2016.

[9] M. Snir, R. W. Wisniewski, J. A. Abraham, S. V. Adve, S. Bagchi, P. Balaji, J. Belak, P. Bose, F. Cappello, B. Carlson *et al.*, "Addressing failures in exascale computing," *The International Journal of High Performance Computing Applications*, vol. 28, no. 2, pp. 129–173, 2014.

[10] D. Oliveira, L. Pilla, N. DeBardeleben, S. Blanchard, H. Quinn, I. Koren, P. Navaux, and P. Rech, "Experimental and analytical study of xeon phi reliability," in *Proceedings of the International Conference for High Performance Computing, Networking, Storage and Analysis*, 2017, pp. 1–12.

[11] L. B. Gomez, F. Cappello, L. Carro, N. DeBardeleben, B. Fang, S. Gurumurthi, K. Pattabiraman, P. Rech, and M. S. Reorda, "Gpgpus: how to combine high computational power with high reliability," in *2014 Design, Automation & Test in Europe Conference & Exhibition (DATE)*. IEEE, 2014, pp. 1–9.

[12] G. Li, S. K. S. Hari, M. Sullivan, T. Tsai, K. Pattabiraman, J. Emer, and S. W. Keckler, "Understanding error propagation in deep learning neural network (dnn) accelerators and applications," in *Proceedings of the International Conference for High Performance Computing, Networking, Storage and Analysis*. ACM, 2017, p. 8.

[13] Z. Chen, G. Li, K. Pattabiraman, and N. DeBardeleben, "Binfi: An efficient fault injector for safety-critical machine learning systems," in *Proceedings of the International Conference for High Performance Computing, Networking, Storage and Analysis*, 2019, pp. 1–23.

[14] C. Schorn, A. Guntoro, and G. Ascheid, "Efficient on-line error detection and mitigation for deep neural network accelerators," in *International Conference on Computer Safety, Reliability, and Security*. Springer, 2018, pp. 205–219.

[15] L.-H. Hoang, M. A. Hanif, and M. Shafique, "Ft-clipact: Resilience analysis of deep neural networks and improving their fault tolerance using clipped activation," *arXiv preprint arXiv:1912.00941*, 2019.

[16] A. Mahmoud, S. K. S. Hari, C. W. Fletcher, S. V. Adve, C. Sakr, N. Shanbhag, P. Molchanov, M. B. Sullivan, T. Tsai, and S. W. Keckler, "Hardnn: Feature map vulnerability evaluation in cnns," *arXiv preprint arXiv:2002.09786*, 2020.

[17] K. Zhao, S. Di, S. Li, X. Liang, Y. Zhai, J. Chen, K. Ouyang, F. Cappello, and Z. Chen, "Algorithm-based fault tolerance for convolutional neural networks," *arXiv preprint arXiv:2003.12203*, 2020.

[18] E. Ozen and A. Orailoglu, "Sanity-check: Boosting the reliability of safety-critical deep neural network applications," in *2019 IEEE 28th Asian Test Symposium (ATS)*. IEEE, 2019, pp. 7–75.

[19] S. Hong, P. Frigo, Y. Kaya, C. Giuffrida, and T. Dumitraş, "Terminal brain damage: Exposing the graceless degradation in deep neural networks under hardware fault attacks," *arXiv preprint arXiv:1906.01017*, 2019.

[20] "Training ai for self-driving vehicles: the challenge of scale." [Online]. Available: https://devblogs.nvidia.com/training-self-driving-vehicles-challenge-scale/

[21] "Autonomous car - a new driver for resilient computing and design-for-test." [Online]. Available: https://nepp.nasa.gov/workshops/etw2016/talks/15WED/20160615-0930-Autonomous_Saxena-Nirmal-Saxena-Rec2016Jun16-nasaNEPP.pdf

[22] M. Abadi, P. Barham, J. Chen, Z. Chen, A. Davis, J. Dean, M. Devin, S. Ghemawat, G. Irving, M. Isard *et al.*, "Tensorflow: A system for large-scale machine learning," in *12th {USENIX} Symposium on Operating Systems Design and Implementation ({OSDI} 16)*, 2016, pp. 265–283.

[23] "Tensorflow popularity." [Online]. Available: https://towardsdatascience.com/deep-learning-framework-power-scores-2018-23607ddf297a

[24] I. Goodfellow, Y. Bengio, A. Courville, and Y. Bengio, *Deep learning*. MIT press, 2016.

[25] J. Langford, L. Li, and T. Zhang, "Sparse online learning via truncated gradient," *Journal of Machine Learning Research*, vol. 10, no. Mar, pp. 777–801, 2009.

[26] Y. Wu and Y. Liu, "Robust truncated hinge loss support vector machines," *Journal of the American Statistical Association*, vol. 102, no. 479, pp. 974–983, 2007.

[27] Z. Ji, Z. C. Lipton, and C. Elkan, "Differential privacy and machine learning: a survey and review," *arXiv preprint arXiv:1412.7584*, 2014.

[28] R. Shokri and V. Shmatikov, "Privacy-preserving deep learning," in *Proceedings of the 22nd ACM SIGSAC conference on computer and communications security*, 2015, pp. 1310–1321.

[29] "Autonomous and adas test cars produce over 11 tb of data per day." [Online]. Available: https://www.tuxera.com/blog/autonomous-and-adas-test-cars-produce-over-11-tb-of-data-per-day/

[30] "Functional safety methodologies for automotive applications." [Online]. Available: https://www.cadence.com/content/dam/cadence-www/global/en_US/documents/solutions/automotive-functional-safety-wp.pdf

[31] K. Pei, Y. Cao, J. Yang, and S. Jana, "Deepxplore: Automated whitebox testing of deep learning systems," in *proceedings of the 26th Symposium on Operating Systems Principles*. ACM, 2017, pp. 1–18.

[32] Y. Tian, K. Pei, S. Jana, and B. Ray, "Deeptest: Automated testing of deep-neural-network-driven autonomous cars," in *Proceedings of the 40th international conference on software engineering*. ACM, 2018, pp. 303–314.

[33] A. H. M. Rubaiyat, Y. Qin, and H. Alemzadeh, "Experimental resilience assessment of an open-source driving agent," *arXiv preprint arXiv:1807.06172*, 2018.

[34] "Yolo v5." [Online]. Available: https://github.com/ultralytics/yolov5.git

[35] S. S. Banerjee, S. Jha, J. Cyriac, Z. T. Kalbarczyk, and R. K. Iyer, "Hands off the wheel in autonomous vehicles?: A systems perspective on over a million miles of field data," in *2018 48th Annual IEEE/IFIP International Conference on Dependable Systems and Networks (DSN)*. IEEE, 2018, pp. 586–597.

[36] B. Reagen, U. Gupta, L. Pentecost, P. Whatmough, S. K. Lee, N. Mulholland, D. Brooks, and G.-Y. Wei, "Ares: A framework for quantifying the resilience of deep neural networks," in *2018 55th ACM/ESDA/IEEE Design Automation Conference (DAC)*. IEEE, 2018, pp. 1–6.

[37] H. Guan, L. Ning, Z. Lin, X. Shen, H. Zhou, and S.-H. Lim, "In-place zero-space memory protection for cnn," *arXiv preprint arXiv:1910.14479*, 2019.

[38] G. Li, K. Pattabiraman, S. K. S. Hari, M. Sullivan, and T. Tsai, "Modeling soft-error propagation in programs," in *2018 48th Annual IEEE/IFIP International Conference on Dependable Systems and Networks (DSN)*. IEEE, 2018, pp. 27–38.

[39] R. A. Ashraf, R. Gioiosa, G. Kestor, R. F. DeMara, C.-Y. Cher, and P. Bose, "Understanding the propagation of transient errors in hpc applications," in *SC'15: Proceedings of the International Conference for High Performance Computing, Networking, Storage and Analysis*. IEEE, 2015, pp. 1–12.

[40] G. Georgakoudis, I. Laguna, D. S. Nikolopoulos, and M. Schulz, "Refine: Realistic fault injection via compiler-based instrumentation for accuracy, portability and speed," in *Proceedings of the International*

Conference for High Performance Computing, Networking, Storage and Analysis. ACM, 2017, p. 29.

[41] B. Fang, K. Pattabiraman, M. Ripeanu, and S. Gurumurthi, "Gpu-qin: A methodology for evaluating the error resilience of gpgpu applications," in *2014 IEEE International Symposium on Performance Analysis of Systems and Software (ISPASS).* IEEE, 2014, pp. 221–230.

[42] J. Wei, A. Thomas, G. Li, and K. Pattabiraman, "Quantifying the accuracy of high-level fault injection techniques for hardware faults," in *2014 44th Annual IEEE/IFIP International Conference on Dependable Systems and Networks.* IEEE, 2014, pp. 375–382.

[43] C.-K. Chang, S. Lym, N. Kelly, M. B. Sullivan, and M. Erez, "Evaluating and accelerating high-fidelity error injection for hpc," in *Proceedings of the International Conference for High Performance Computing, Networking, Storage, and Analysis*, ser. SC '18, 2018, pp. 45:1–45:13.

[44] B. Sangchoolie, K. Pattabiraman, and J. Karlsson, "One bit is (not) enough: An empirical study of the impact of single and multiple bit-flip errors," in *2017 47th Annual IEEE/IFIP International Conference on Dependable Systems and Networks (DSN).* IEEE, 2017, pp. 97–108.

[45] C.-K. Chang, S. Lym, N. Kelly, M. B. Sullivan, and M. Erez, "Evaluating and accelerating high-fidelity error injection for hpc," in *Proceedings of the International Conference for High Performance Computing, Networking, Storage, and Analysis.* IEEE Press, 2018, p. 45.

[46] S. Venkataramani, A. Ranjan, K. Roy, and A. Raghunathan, "Axnn: Energy-efficient neuromorphic systems using approximate computing," in *2014 IEEE/ACM International Symposium on Low Power Electronics and Design (ISLPED).* IEEE, 2014, pp. 27–32.

[47] S. K. S. Hari, S. V. Adve, H. Naeimi, and P. Ramachandran, "Relyzer: Exploiting application-level fault equivalence to analyze application resiliency to transient faults," in *ACM SIGPLAN Notices*, vol. 47, no. 4. ACM, 2012, pp. 123–134.

[48] G. Li, K. Pattabiraman, and N. DeBardeleben, "Tensorfi: A configurable fault injector for tensorflow applications," in *2018 IEEE International Symposium on Software Reliability Engineering Workshops (ISSREW).* IEEE, 2018, pp. 313–320.

[49] "comma.ai's steering model." [Online]. Available: https://github.com/commaai/research

[50] "On-road tests for nvidia dave system." [Online]. Available: https://devblogs.nvidia.com/deep-learning-self-driving-cars/

[51] "Driving dataset." [Online]. Available: https://github.com/SullyChen/driving-datasets

[52] S. Du, H. Guo, and A. Simpson, "Self-driving car steering angle prediction based on image recognition," *Department of Computer Science, Stanford University, Tech. Rep. CS231-626*, 2017.

[53] "Tensorflow implementation of nvidia dave system." [Online]. Available: https://github.com/SullyChen/Autopilot-TensorFlow

[54] P. Judd, J. Albericio, T. Hetherington, T. Aamodt, N. E. Jerger, R. Urtasun, and A. Moshovos, "Proteus: Exploiting precision variability in deep neural networks," *Parallel Computing*, 2018.

[55] R. Tang, W. Wang, Z. Tu, and J. Lin, "An experimental analysis of the power consumption of convolutional neural networks for keyword spotting," in *2018 IEEE International Conference on Acoustics, Speech and Signal Processing (ICASSP).* IEEE, 2018, pp. 5479–5483.

[56] S. Han, J. Pool, J. Tran, and W. Dally, "Learning both weights and connections for efficient neural network," in *Advances in neural information processing systems*, 2015, pp. 1135–1143.

[57] A. Sehgal and N. Kehtarnavaz, "Guidelines and benchmarks for deployment of deep learning models on smartphones as real-time apps," *Machine Learning and Knowledge Extraction*, vol. 1, no. 1, pp. 450–465, 2019.

[58] L. Yang, B. Nie, A. Jog, and E. Smirni, "Practical resilience analysis of gpgpu applications in the presence of single- and multi-bit faults," *IEEE Transactions on Computers*, vol. 70, no. 01, pp. 30–44, jan 2021.

[59] B. Reagen, P. Whatmough, R. Adolf, S. Rama, H. Lee, S. K. Lee, J. M. Hernández-Lobato, G.-Y. Wei, and D. Brooks, "Minerva: Enabling low-power, highly-accurate deep neural network accelerators," in *ACM/IEEE 43rd Annual International Symposium on Computer Architecture (ISCA).* IEEE, 2016.

[60] F. F. dos Santos, C. Lunardi, D. Oliveira, F. Libano, and P. Rech, "Reliability evaluation of mixed-precision architectures," in *2019 IEEE International Symposium on High Performance Computer Architecture (HPCA).* IEEE, 2019, pp. 238–249.

[61] S. K. S. Hari, M. B. Sullivan, T. Tsai, and S. W. Keckler, "Making convolutions resilient via algorithm-based error detection techniques," *arXiv preprint arXiv:2006.04984*, 2020.

[62] F. F. dos Santos, P. F. Pimenta, C. Lunardi, L. Draghetti, L. Carro, D. Kaeli, and P. Rech, "Analyzing and increasing the reliability of convolutional neural networks on gpus," *IEEE Transactions on Reliability*, vol. 68, no. 2, pp. 663–677, 2018.

[63] M. A. Hanif, R. Hafiz, and M. Shafique, "Error resilience analysis for systematically employing approximate computing in convolutional neural networks," in *2018 Design, Automation & Test in Europe Conference & Exhibition (DATE).* IEEE, 2018.

[64] N. Papernot, P. McDaniel, A. Sinha, and M. P. Wellman, "Sok: Security and privacy in machine learning," in *2018 IEEE European Symposium on Security and Privacy (EuroS&P).* IEEE, 2018, pp. 399–414.